

This article was downloaded by:

On: 25 January 2011

Access details: *Access Details: Free Access*

Publisher *Taylor & Francis*

Informa Ltd Registered in England and Wales Registered Number: 1072954 Registered office: Mortimer House, 37-41 Mortimer Street, London W1T 3JH, UK



## Liquid Crystals

Publication details, including instructions for authors and subscription information:

<http://www.informaworld.com/smpp/title~content=t713926090>

### Monohalocyclohexanes in liquid crystalline solution: the molecular behaviour of chloro- and iodo-cyclohexane

Sabine Ternieden<sup>a</sup>; Diana Zauser<sup>a</sup>; Klaus Müller<sup>a</sup>

<sup>a</sup> Institut für Physikalische Chemie, Universität Stuttgart, Pfaffenwaldring 55, D-70569 Stuttgart, Germany,

Online publication date: 06 August 2010

**To cite this Article** Ternieden, Sabine , Zauser, Diana and Müller, Klaus(2000) 'Monohalocyclohexanes in liquid crystalline solution: the molecular behaviour of chloro- and iodo-cyclohexane', *Liquid Crystals*, 27: 9, 1171 – 1182

**To link to this Article:** DOI: 10.1080/02678290050122015

**URL:** <http://dx.doi.org/10.1080/02678290050122015>

PLEASE SCROLL DOWN FOR ARTICLE

Full terms and conditions of use: <http://www.informaworld.com/terms-and-conditions-of-access.pdf>

This article may be used for research, teaching and private study purposes. Any substantial or systematic reproduction, re-distribution, re-selling, loan or sub-licensing, systematic supply or distribution in any form to anyone is expressly forbidden.

The publisher does not give any warranty express or implied or make any representation that the contents will be complete or accurate or up to date. The accuracy of any instructions, formulae and drug doses should be independently verified with primary sources. The publisher shall not be liable for any loss, actions, claims, proceedings, demand or costs or damages whatsoever or howsoever caused arising directly or indirectly in connection with or arising out of the use of this material.

# Monohalocyclohexanes in liquid crystalline solution: the molecular behaviour of chloro- and iodo-cyclohexane

SABINE TERNIEDEN, DIANA ZAUSER and KLAUS MÜLLER\*

Institut für Physikalische Chemie, Universität Stuttgart, Pfaffenwaldring 55,  
D-70569 Stuttgart, Germany

(Received 26 January 2000; accepted 10 March 2000)

Dynamic  $^2\text{H}$  NMR spectroscopy is used to study selectively and perdeuteriated samples of chloro- and iodo-cyclohexane dissolved in a liquid crystalline solution. The equatorial and axial conformers are found to exist in a dynamic equilibrium with relative amounts of about  $p_e = 0.7$  and  $p_a = 0.3$ , respectively, as taken from the  $^2\text{H}$  NMR lineshapes and 2D exchange spectra. The quantitative analysis of variable temperature  $^2\text{H}$  NMR spectra provides the kinetic parameters of the underlying ring inversion process. The activation enthalpies of this internal process are given by  $\Delta H = 48.1 \pm 1.0$  and  $40.6 \pm 2.3 \text{ kJ mol}^{-1}$  for chloro- and iodo-cyclohexane, respectively. These values resemble those reported from earlier studies of isotropic solutions. The molecular order parameters, as well as the orientation of the main ordering axis, for the axial and equatorial conformers are determined as functions of temperature. These molecular quantities exhibit a strong dependence on the actual conformational state and size of the substituent, while polar effects of the substituents seem to play no important role.

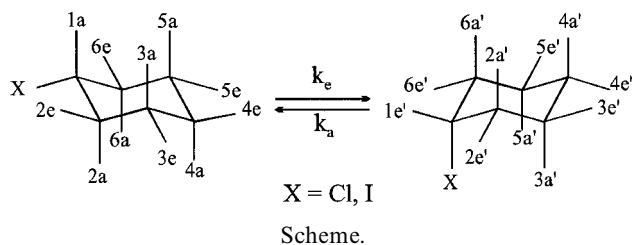
## 1. Introduction

During recent years, knowledge about the molecular behaviour of liquid crystalline systems has increased substantially on the basis of both theoretical and experimental studies. Here, NMR spectroscopy has shown its particular suitability, since the analysis of NMR lineshapes and relaxation data could provide detailed information about the molecular order and dynamics of such anisotropic phases [1–3]. Investigations have thus been performed to unravel the properties of the liquid crystal forming compounds [4–8], as well as the molecular features of guest molecules dissolved in various types of liquid crystalline solvent [9–13]. In this connection, solute molecules of quite different chemical structures and flexibility have been examined [14–25]. The analysis of dynamic  $^1\text{H}$ ,  $^2\text{H}$  or  $^{13}\text{C}$  NMR experiments—including lineshape, relaxation and 2D exchange measurements—have given access to the ordering behaviour of such solutes, as well as their dynamical characteristics in terms of internal and overall types of motion. Recently,  $^2\text{H}$  NMR techniques have been employed successfully for the characterization of deuteriated cyclohexane derivatives with either non-polar or polar substituents in liquid crystalline (nematic) solvents [21–25]. In those cases with two coexisting conformers, the observed  $^2\text{H}$  NMR lineshape changes were found to reflect the ring inversion

process, i.e. mutual exchange of the two conformational states. The derived kinetic parameters, i.e. rate constants and activation energies, of the ring inversion process generally were found to be almost unaffected by the liquid crystal solvent. On the other hand, the ordering characteristics—in terms of the molecular order parameters—displayed a strong dependence on the actual chemical structure of the cyclohexane derivatives. The case of bromocyclohexane was unique in the sense that a polar substituent was present and that two conformers of different structures and amounts coexist [25]. Moreover, the derived molecular order parameters were found to vary considerably with the actual conformational state, which was traced back to different overall shapes of the conformers.

The intention of the present contribution is to provide further experimental data for liquid crystalline solutes bearing polar substituents. To do so, we have performed  $^2\text{H}$  NMR measurements on selectively and perdeuteriated chloro- and iodo-cyclohexane dissolved in the nematic mixture ZLI 2452, comprising variable temperature lineshape studies, as well as 2D exchange experiments. The analysis of these experimental data has provided the rate constants and activation energies of the ring inversion process (see the scheme), the relative amounts of the equatorial and axial conformers and—with the known geometry from molecular mechanics calculations—the molecular order parameters of the coexisting equatorial and axial conformers. The derived results are further discussed by considering earlier studies on related systems.

\* Author for correspondence  
e-mail: k.mueller@ipc.uni-stuttgart.de



## 2. Experimental

### 2.1. Materials

All chemicals for the synthesis of deuteriated chloro- and iodo-cyclohexane were obtained from Aldrich Chemicals (Steinheim/Germany). The nematic mixture ZLI 2452 (Merck, Darmstadt) served as the liquid crystalline solvent exhibiting a nematic range between 233 and 383 K. For the NMR measurements, solutions containing 3–5 wt % of deuteriated chloro- or iodo-cyclohexane were sealed in 5 mm NMR tubes.

### 2.2. Synthesis

In this section, we briefly describe the synthetic routes for the preparation of selectively and perdeuteriated chloro- and iodo-cyclohexanes. Further details are given in the cited references.

#### 2.2.1. Cyclohexanone-2,2,6,6-*d*<sub>4</sub>

Cyclohexanone-2,2,6,6-*d*<sub>4</sub> was synthesized by basic H/D exchange of cyclohexanone in D<sub>2</sub>O with a catalytic amount of Na<sub>2</sub>CO<sub>3</sub> [26]. The mixture was stirred for 8 h at 80°C and washed with ether. The organic layer was dried and the solvent evaporated. The crude product was used as starting material for a new exchange cycle. After three cycles of exchange the product was distilled in vacuum. The total yield was 55% of product with ≥ 95% of deuteration at positions C-2 and C-6.

#### 2.2.2. Cyclohexanol-2,2,6,6-*d*<sub>4</sub>

Cyclohexanone-2,2,6,6-*d*<sub>4</sub> in ether was slowly added to an ethereal solution of LiAlH<sub>4</sub> under a nitrogen atmosphere [27]. The mixture was then heated at reflux for 8 h and stirred at room temperature for 12 h. After careful hydrolysis, the precipitate was dissolved in 5% H<sub>2</sub>SO<sub>4</sub> and the mixture was shaken with ether. The organic phase was separated, washed with aqueous NaHCO<sub>3</sub>, dried and evaporated. The product was distilled in vacuum; yield 76%.

#### 2.2.3. Cyclohexanol-1-*d*<sub>1</sub>

Here, the same procedure was applied as that described in §2.2.2. for cyclohexanol-2,2,6,6-*d*<sub>4</sub>, except that the reaction was performed with cyclohexanone and LiAlD<sub>4</sub>, yield 70%.

#### 2.2.4. Chlorocyclohexane-1-*d*<sub>1</sub>

Cyclohexanol-1-*d*<sub>1</sub> in chloroform was cooled using an ice bath. After careful addition of PCl<sub>5</sub>, the mixture was stirred for 3 h at low temperature and for 18 h at room temperature [28]. After hydrolysis with water (with cooling), the mixture was stirred for another 18 h. The product was separated from unwanted 1,2-*trans*-dichlorocyclohexane by distillation; yield 28%.

#### 2.2.5. Chlorocyclohexane-2,2,6,6-*d*<sub>4</sub>

Here, the same procedure was employed as for the synthesis of chlorocyclohexane-1-*d*<sub>1</sub>, except that cyclohexanol-2,2,6,6-*d*<sub>4</sub> was used instead of cyclohexanol-1-*d*<sub>1</sub>; the yield was 27%.

#### 2.2.6. Chlorocyclohexane-*d*<sub>11</sub>

After addition of DCl to cyclohexanol-*d*<sub>11</sub> at room temperature the mixture was stirred for 3 h under reflux, followed by 12 h at room temperature [29]. The mixture was then shaken with ether, and the ethereal phase was washed with aqueous Na<sub>2</sub>CO<sub>3</sub>, H<sub>2</sub>O and dried over CaCl<sub>2</sub>. After removing the solvent, the product was purified via column chromatography using a *n*-hexane CHCl<sub>3</sub> (1/1) mixture; the yield was 20%. As shown below, the product still contained a considerable amount of cyclohexanol-*d*<sub>11</sub>.

#### 2.2.7. Iodocyclohexane-2,2,6,6-*d*<sub>4</sub>

In the first step, H<sub>3</sub>PO<sub>4</sub> and KI were mixed in the cold using an ice bath [30]. The mixture was then warmed up to room temperature and cyclohexanol-2,2,6,6-*d*<sub>4</sub> was slowly added, followed by stirring for 6 h at 110°C and 12 h at room temperature. After addition of water and ether, the ethereal phase was washed with aqueous Na<sub>2</sub>S<sub>2</sub>O<sub>3</sub> (until colourless) and aqueous NaCl, followed by drying over Na<sub>2</sub>SO<sub>4</sub>. The solvent was removed and the crude product purified by column chromatography (solvent *n*-hexane) giving a yield of 48%. In the high resolution <sup>13</sup>C NMR spectra of iodocyclohexane-2,2,6,6-*d*<sub>4</sub>, signals from by-products showed up. By analogy with the previous work on bromocyclohexane, they could be attributed to iodocyclohexane, deuteriated at C-1 and C-3/C-5 due to a competing addition/elimination reaction [25].

#### 2.2.8. Iodocyclohexane-*d*<sub>11</sub>

The procedure of §2.2.7 was employed using perdeuteriated cyclohexanol-*d*<sub>11</sub> as starting compound; the yield was 45%.

## 2.3. NMR measurements

All <sup>2</sup>H NMR measurements were performed using a Bruker CXP 300 NMR spectrometer (Rheinstetten/Germany), equipped with a Tecmag control unit

(Houston, USA), operating at 46.07 MHz for deuterium.  $^2\text{H}$  NMR spectra were recorded employing the quadrupole echo sequence  $(\pi/2)_x-\tau_1-(\pi/2)_y-\tau_2$  with a  $(\pi/2)$  pulse length of  $2\ \mu\text{s}$  and a pulse spacing of  $\tau_1 = \tau_2 = 20\ \mu\text{s}$ . The number of scans varied between 256 and 2048. Recycle delays were chosen to be at least five times  $T_1$ , ranging from 1 to 5 s. 2D exchange  $^2\text{H}$  NMR experiments were performed with a five-pulse version [31] of the original experiment and a mixing time of 3 ms. A spectral width of 100 kHz in both dimensions and 128  $t_1$  values were used to collect two separate data sets (cos- and sin-part), which were processed as previously described [32]. The sample temperature during the  $^2\text{H}$  NMR experiments was controlled with a Bruker BVT 2000 unit with a temperature stability of  $\pm 0.2\ \text{K}$ .

#### 2.4. Molecular mechanics calculations

The molecular coordinates of the chloro- and iodo-cyclohexane conformers were determined with the MM2 programme [33], implemented in the SYBYL software package (Tripos, St. Louis/USA). Tables 1 and 2 summarize the coordinates in the molecule fixed coordinate system  $x'$ ,  $y'$ ,  $z'$ . The molecular  $x'$ -axis lies along the C-6/C-5 axis and the  $x'$ ,  $y'$ -plane is defined by C-5, C-6 and C-2 (see figure 1). The quality of the derived molecular geometry data was checked by a comparison with the structures derived by gas phase electron diffraction, microwave spectroscopy and *ab initio* calculation [34–36]. The theoretical and experimental geometries were in very good agreement, exhibiting deviations less than  $0.02\ \text{\AA}$  (bond lengths) and  $1^\circ$  (bond angles).

#### 2.5. Simulations

The data processing of the experimental and simulated NMR signals was performed on a SUN Sparc 10 workstation using the NMRi and SYBYL software packages (Tripos, St. Louis/USA). Lineshape simulations for an  $I = 1$  spin system, taking into account two-site exchange and the relaxation delay  $\tau$  in the quadrupole echo experiment, were done with an appropriate FORTRAN programme [25]. The best fit  $^2\text{H}$  NMR spectra were obtained by visual inspection of the experimental spectra and their theoretical counterparts.

### 3. Results and discussion

Selectively and perdeuterated chloro- and iodo-cyclohexanes, dissolved in the liquid crystalline solution ZLI 2452, were studied by  $^2\text{H}$  NMR spectroscopy. The typical 'single crystal'-like  $^2\text{H}$  NMR spectra can be understood by the fact that the liquid crystal domains are aligned by the strong external magnetic field [1–3]. The macroscopic alignment of the liquid crystalline matrix is further transferred to the solute molecules via intermolecular interactions. The presence of fast overall motions of the oriented solute molecules then gives rise to motionally averaged  $^2\text{H}$  NMR spectra, as expressed by a reduced quadrupolar splitting  $2\langle \Delta\nu_Q \rangle$ . The  $^2\text{H}$  NMR spectra and relaxation data can be further analysed in terms of internal and overall dynamic processes and the solute ordering characteristics, as will be outlined below.

#### 3.1. $^2\text{H}$ NMR spectra and spectral assignment

This section deals with the appearance of the experimental  $^2\text{H}$  NMR spectra of chloro- and iodo-cyclohexane

Table 1. Coordinates of the carbon and deuterium atoms in chlorocyclohexane as derived from molecular mechanics calculations (MM2 force field [33]).

| Atom | Equatorial conformer |                 |                 | Atom  | Axial conformer |                 |                 |
|------|----------------------|-----------------|-----------------|-------|-----------------|-----------------|-----------------|
|      | $x'/\text{\AA}$      | $y'/\text{\AA}$ | $z'/\text{\AA}$ |       | $x'/\text{\AA}$ | $y'/\text{\AA}$ | $z'/\text{\AA}$ |
| C-1  | -0.541               | 0.699           | 0.000           | C-1'  | -0.541          | 0.699           | 0.000           |
| C-2  | 0.000                | 0.000           | 1.274           | C-2'  | 0.000           | 0.000           | 1.274           |
| C-3  | 1.551                | 0.000           | 1.274           | C-3'  | 1.551           | 0.000           | 1.274           |
| C-4  | 2.092                | -0.699          | 0.000           | C-4'  | 2.092           | -0.699          | 0.000           |
| C-5  | 1.550                | 0.000           | -1.274          | C-5'  | 1.551           | 0.000           | -1.274          |
| C-6  | 0.000                | 0.000           | -1.274          | C-6'  | 0.000           | 0.000           | -1.274          |
| D-1a | -0.233               | 1.758           | 0.000           | D-1e' | -1.644          | 0.668           | 0.000           |
| D-2a | -0.369               | -1.038          | 1.306           | D-2a' | -0.368          | -1.039          | 1.308           |
| D-2e | -0.371               | 0.525           | 2.169           | D-2e' | -0.371          | 0.524           | 2.170           |
| D-3a | 1.919                | 1.039           | 1.309           | D-3a' | 1.919           | 1.039           | 1.309           |
| D-3e | 1.921                | -0.525          | 2.171           | D-3e' | 1.922           | -0.524          | 2.171           |
| D-4a | 1.783                | -1.757          | 0.000           | D-4a' | 1.781           | -1.757          | 0.000           |
| D-4e | 3.195                | -0.666          | 0.000           | D-4e' | 3.195           | -0.668          | 0.000           |
| D-5a | 1.919                | 1.039           | -1.309          | D-5a' | 1.919           | 1.039           | -1.309          |
| D-5e | 1.921                | -0.525          | -2.171          | D-5e' | 1.922           | -0.524          | -2.171          |
| D-6a | -0.369               | -1.038          | -1.306          | D-6a' | -0.368          | -1.039          | -1.308          |
| D-6e | -0.371               | 0.525           | -2.169          | D-6e' | -0.371          | 0.524           | -2.170          |

Table 2. Coordinates of the carbon and deuterium atoms in iodocyclohexane as derived from molecular mechanics calculations (MM2 force field [33]).

| Atom | Equatorial conformer |                 |                 | Atom  | Axial conformer |                 |                 |
|------|----------------------|-----------------|-----------------|-------|-----------------|-----------------|-----------------|
|      | $x'/\text{\AA}$      | $y'/\text{\AA}$ | $z'/\text{\AA}$ |       | $x'/\text{\AA}$ | $y'/\text{\AA}$ | $z'/\text{\AA}$ |
| C-1  | -0.542               | 0.698           | 0.000           | C-1'  | -0.567          | 0.674           | 0.000           |
| C-2  | 0.000                | 0.000           | 1.274           | C-2'  | 0.000           | 0.000           | 1.274           |
| C-3  | 1.550                | 0.000           | 1.274           | C-3'  | 1.556           | 0.000           | 1.274           |
| C-4  | 2.092                | -0.699          | 0.000           | C-4'  | 2.093           | -0.701          | 0.000           |
| C-5  | 1.551                | 0.000           | -1.274          | C-5'  | 1.556           | 0.000           | -1.274          |
| C-6  | 0.000                | 0.000           | -1.274          | C-6'  | 0.000           | 0.000           | -1.274          |
| D-1a | -0.234               | 1.757           | 0.000           | D-1e' | -1.665          | 0.570           | 0.000           |
| D-2a | -0.369               | -1.038          | 1.308           | D-2a' | -0.353          | -1.042          | 1.326           |
| D-2e | -0.373               | 0.525           | 2.169           | D-2e' | -0.366          | 0.528           | 2.173           |
| D-3a | 1.918                | 1.039           | 1.310           | D-3a' | 1.937           | 1.033           | 1.313           |
| D-3e | 1.920                | -0.523          | 2.169           | D-3e' | 1.926           | -0.529          | 2.170           |
| D-4a | 1.780                | -1.757          | 0.000           | D-4a' | 1.779           | -1.757          | 0.000           |
| D-4e | 3.194                | -0.668          | 0.000           | D-4e' | 3.196           | -0.673          | 0.000           |
| D-5a | 1.918                | 1.039           | -1.310          | D-5a' | 1.937           | 1.033           | -1.313          |
| D-5e | 1.920                | -0.523          | -2.169          | D-5e' | 1.926           | -0.529          | -2.170          |
| D-6a | -0.369               | -1.038          | -1.308          | D-6a' | -0.353          | -1.042          | -1.326          |
| D-6e | -0.373               | 0.525           | -2.169          | D-6e' | -0.366          | 0.528           | -2.173          |

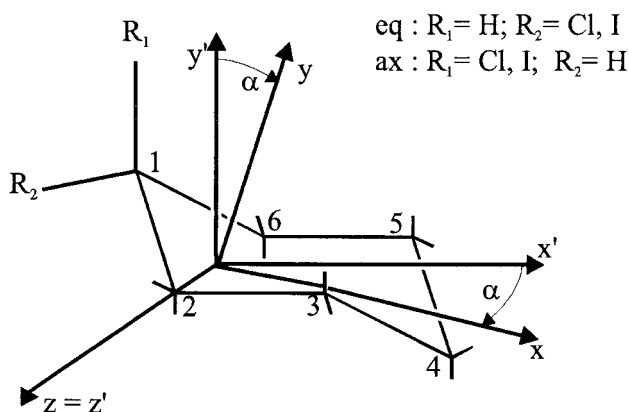


Figure 1. Definitions of coordinate systems used during the present study. The molecular-fixed system is given by  $x'$  and  $y'$  in the symmetry plane of the molecule;  $z'$  is perpendicular to the symmetry plane. The origin is halfway between carbons C-2 and C-6. The principal axis system  $x, y, z$  is related to the molecular-fixed system by a rotation through an angle  $\alpha$  about  $z' = z$ .

and the assignment of the individual NMR signals in the liquid crystalline solution ZLI 2452 that is based on the analysis of variable temperature NMR spectra, as well as 2D exchange NMR spectra.

### 3.1.1. Chlorocyclohexane

To begin with we present the results from three samples with deuteriated chlorocyclohexane, namely chlorocyclohexane-1-d<sub>1</sub>, chlorocyclohexane-2,2,6,6-d<sub>4</sub> and chlorocyclohexane-d<sub>11</sub>. We follow here the procedure that has been discussed extensively in the preceding paper on bromocyclohexane [25]. Figure 2 contains

variable temperature <sup>2</sup>H NMR lineshapes of chlorocyclohexane-1-d<sub>1</sub> in the liquid crystalline solvent ZLI 2452. Inspection of this figure reveals that at 238 K the <sup>2</sup>H NMR spectrum is given by a superposition of two doublets. They reflect the deuterons at carbon C-1 in the equatorial (D-1a: 25.4 kHz) and axial (D-1e': 4.3 kHz) conformational state. Furthermore, from the line intensities a relative population of the equatorial conformer with  $p_e = 0.72$  has been derived, being almost identical with the values reported from studies using an isotropic solution [37–39]. Upon further increase of the sample temperature, a substantial line broadening is registered. Eventually, at higher temperatures the lines merge, resulting in a single quadrupolar doublet above 283 K. This behaviour can be understood by the presence of the well known ring inversion process. Accidentally, the rate constants of this process match the sensitive range of the <sup>2</sup>H NMR lineshapes, giving rise to such spectral effects. The theoretical <sup>2</sup>H NMR spectra, given in the right column of figure 2, have been obtained on the basis of this internal process (see also discussion below). At 333 K the ring inversion is in the fast exchange limit, as expressed by a single <sup>2</sup>H doublet of reduced linewidth which is the weighted sum of the individual doublets of the two chlorocyclohexane conformers.

The <sup>2</sup>H NMR lineshapes and the 2D exchange <sup>2</sup>H NMR spectrum given in figures 3 and 4, refer to chlorocyclohexane-2,2,6,6-d<sub>4</sub> in ZLI 2452. At 238 K four doublets are visible that can be attributed to the two deuterons of the CD<sub>2</sub> group in the equatorial and axial conformers. Since chlorocyclohexane possesses a plane of symmetry, the deuterons at carbon C-2 and C-6 should

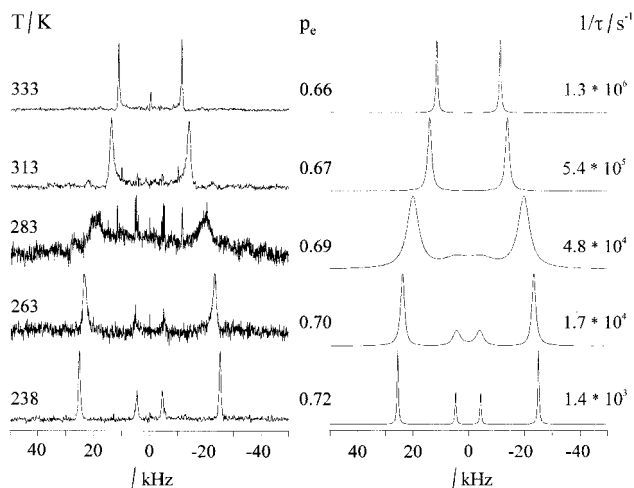


Figure 2. Experimental (left column) and simulated (right column)  $^2\text{H}$  NMR spectra of chlorocyclohexane-1- $\text{d}_1$  at various temperatures. The rate constants for the ring inversion process and the relative amounts of equatorial conformers are given in the figure.

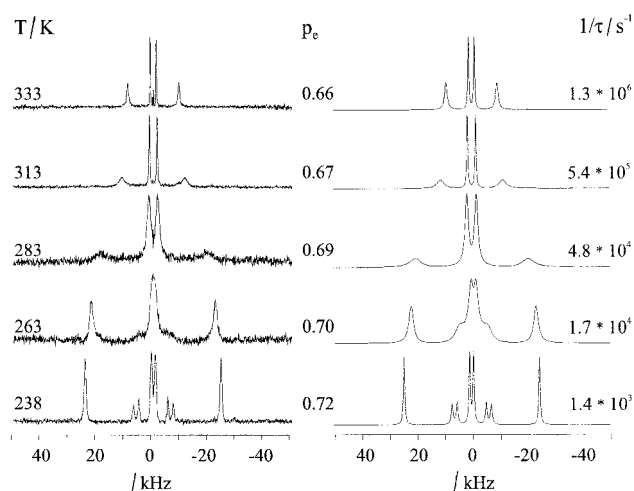


Figure 3. Experimental (left column) and simulated (right column)  $^2\text{H}$  NMR spectra of chlorocyclohexane-2,2,6,6- $\text{d}_4$  at various temperatures. The rate constants for the ring inversion process and the relative amounts of equatorial conformers are given in the figure.

be magnetically equivalent. Again, the signal intensities at low temperatures provided the relative populations of the two coexisting conformers while the lineshape effects at higher temperatures reflect the presence of the ring inversion process. As outlined previously [21–25], the presence of the ring inversion process can also be studied by the 2D exchange NMR spectrum, given in figure 4. Here, the observed cross peaks connect those  $^2\text{H}$  doublets that are exchanged due to the internal ring inversion process. In addition, the 2D exchange NMR

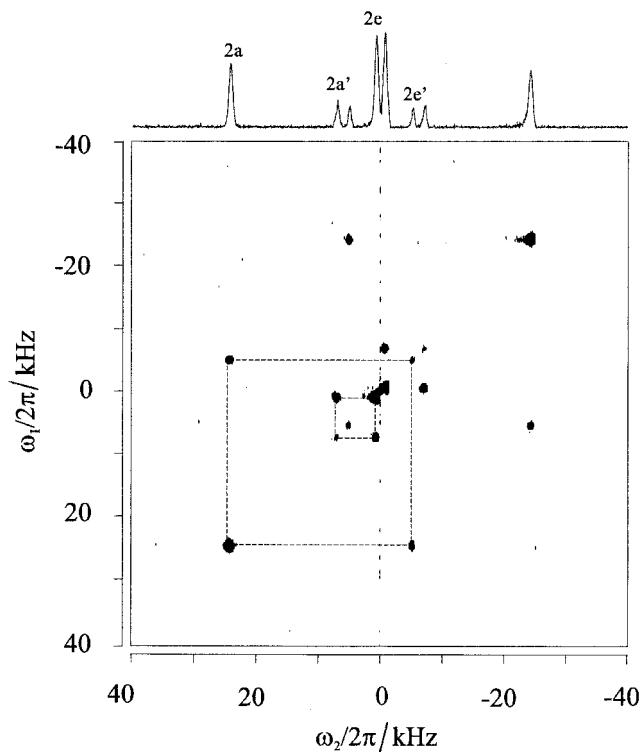


Figure 4. 2D exchange  $^2\text{H}$  NMR spectrum of chlorocyclohexane-2,2,6,6- $\text{d}_4$ , recorded at 238 K with a mixing time of 3 ms.

spectrum contains information about the relative signs of the (averaged) quadrupolar couplings of the interchanging signals [21, 22]. This information is of great importance for the determination of the absolute signs of the averaged quadrupolar couplings and molecular order parameters of the solutes (see below). Inspection of the 2D exchange NMR spectrum of chlorocyclohexane-2,2,6,6- $\text{d}_4$  reveals that one pair of signals possesses opposite signs (at 25.3 and 5.0 kHz), while the second pair exhibits the same relative signs (0.8 and 7.8 kHz) for the quadrupolar couplings. The signals of lower intensity (5.0 and 7.8 kHz) were attributed to the axial conformer, and those of higher intensity to the equatorial conformer. Comparison with published data for bromocyclohexane [25] further suggested the following assignment: D-2a/D-2e' at 25.3/5.0 kHz and D-2e/D-2a' at 0.8/7.8 kHz.

The remaining signals due to the deuterons at C-3 and C-4 were derived from the experiments on perdeuterated chlorocyclohexane- $\text{d}_{11}$ . The variable temperature  $^2\text{H}$  NMR lineshapes and the 2D exchange  $^2\text{H}$  NMR spectrum of this compound are given in figures 5 and 6. Due to the  $C_s$  symmetry of chlorocyclohexane, the maximum number of signal doublets for each conformer should be seven. The spectral analysis, however, revealed that the actual number of doublets is lower due to some

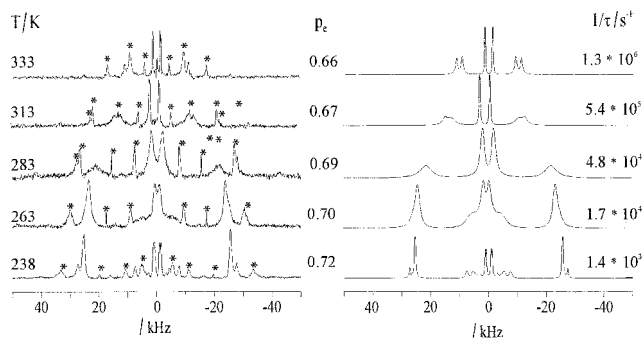


Figure 5. Experimental (left column) and simulated (right column)  $^2\text{H}$  NMR spectra of chlorocyclohexane- $\text{d}_{11}$  at various temperatures. Asterisks indicate signals due to cyclohexanol- $\text{d}_{11}$ . The rate constants for the ring inversion process and the relative amounts of equatorial conformers are given in the figure.

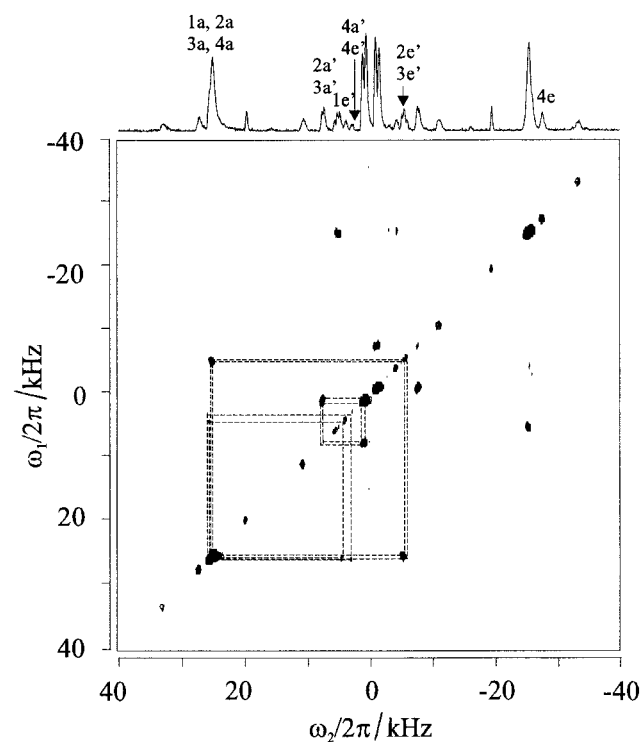


Figure 6. 2D exchange  $^2\text{H}$  NMR spectrum of chlorocyclohexane- $\text{d}_{11}$ , recorded at 238 K with a mixing time of 3 ms.

spectral overlap. On the other hand, additional signals—indicated by asterisks in figure 5—were registered that do not belong to chlorocyclohexane- $\text{d}_{11}$ . Rather they stem from remaining cyclohexanol- $\text{d}_{11}$  that was not separated during the chemical synthesis and subsequent purification. Again, the cross peaks in the 2D exchange  $^2\text{H}$  NMR spectrum at 238 K were used to determine the quadrupolar doublets of the remaining deuterons at C-3 and C-4 as well as the relative signs of their averaged coupling constants. The final assignment of these signals

to a specific C–D bond, however, could not be done unequivocally. To do so, the molecular geometry from the MM2 calculations [33] had to be taken into account in the same way as before on related compounds [21–25]. It should be mentioned that the cross peaks between the D-4e and D-4a' signals were not detectable in the experimental 2D exchange  $^2\text{H}$  NMR spectrum. Their assignment was feasible during the 1D lineshape and order parameter analysis. In addition, the previous assignments from the study on bromocyclohexane were taken into account [25].

### 3.1.2. Iodocyclohexane

Similar  $^2\text{H}$  NMR studies were performed for the samples of iodocyclohexane in ZLI 2452. In figures 7 and 8 variable temperature  $^2\text{H}$  NMR spectra of the sample with iodocyclohexane-2,2,6,6- $\text{d}_4$  are given. The analysis of these spectra, however, revealed that the sample contained iodocyclohexane-2,2,6,6- $\text{d}_4$ , as well as iodocyclohexane-1,3,3- $\text{d}_3$  and iodocyclohexane-*cis*-2,6,6- $\text{d}_3$  in a molar ratio 1:1:1. The latter by-products were attributed to a competing elimination/addition situation during the final step of the chemical synthesis in just the same way as discussed earlier for bromocyclohexane. That is, cyclohexene is formed as a reaction intermediate, followed by an attack of HI at the C=C bond giving rise to the above-mentioned by-products [25]. In the present case, the addition/elimination reactions even dominated the substitution reaction, as expressed by the ratio of elimination to substitution products of 2:1. As before, the changes in the variable temperature

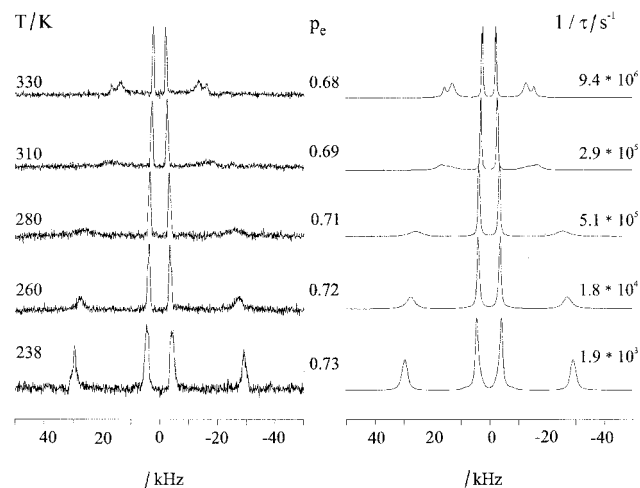


Figure 7. Experimental (left column) and simulated (right column)  $^2\text{H}$  NMR spectra of iodocyclohexane-2,2,6,6- $\text{d}_4$  at various temperatures. The rate constants for the ring inversion process and the relative amounts of equatorial conformers are given in the figure. As discussed in the text, the sample also contains iodocyclohexane-*cis*-2,6,6- $\text{d}_3$  and iodocyclohexane-1,3,3- $\text{d}_3$ .

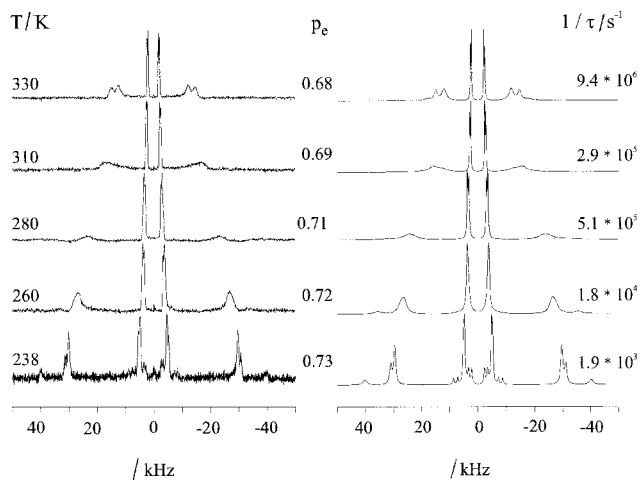


Figure 8. Experimental (left column) and simulated (right column)  $^2\text{H}$  NMR spectra of iodocyclohexane- $\text{d}_{11}$  at various temperatures. The rate constants for the ring inversion process and the relative amounts of equatorial conformers are given in the figure.

$^2\text{H}$  NMR spectra reflect the presence of the ring inversion process. Their analysis provided the populations of the equatorial and axial conformers as well as the rate constants of the ring inversion process. At 238 K the population of the equatorial conformer was  $p_e = 0.73$  which again is very close to the values in isotropic solution [37, 39]. Figures 8 and 9 display variable temperature  $^2\text{H}$  NMR spectra and a 2D exchange  $^2\text{H}$  NMR spectrum at 238 K for perdeuteriated iodocyclohexane- $\text{d}_{11}$ . Unlike the previous case of chlorocyclohexane- $\text{d}_{11}$ , no disturbing signals from cyclohexanol- $\text{d}_{11}$  were registered for the sample of iodocyclohexane- $\text{d}_{11}$ . From the analysis of both the 1D lineshapes and the 2D exchange  $^2\text{H}$  NMR spectrum, the remaining signal pairs (undergoing chemical exchange) and the relative signs of the quadrupolar couplings could be determined. Again, it should be noted that the cross peaks between the D-4e and D-4a' signals were missing in the 2D exchange NMR spectrum. They were identified and finally assigned by proceeding in the same way as for chlorocyclohexane in ZLI 2452.

### 3.2. Molecular ordering

The final assignment of all  $^2\text{H}$  NMR doublets and the determination of the ordering matrix for chloro- and iodo-cyclohexane in the nematic mixture ZLI 2452 was achieved using a procedure that has been outlined previously and that will now be described briefly. The solute molecules studied here possess  $C_s$  symmetry. For this reason, three Euler angles—connecting the molecular-fixed coordinate system ( $x', y', z'$ ) and the principal axes system of the ordering matrix ( $x, y, z$ )—as well as the order parameters  $S_{xx}, S_{yy}, S_{zz}$  [40] in the  $x, y, z$  coordinate

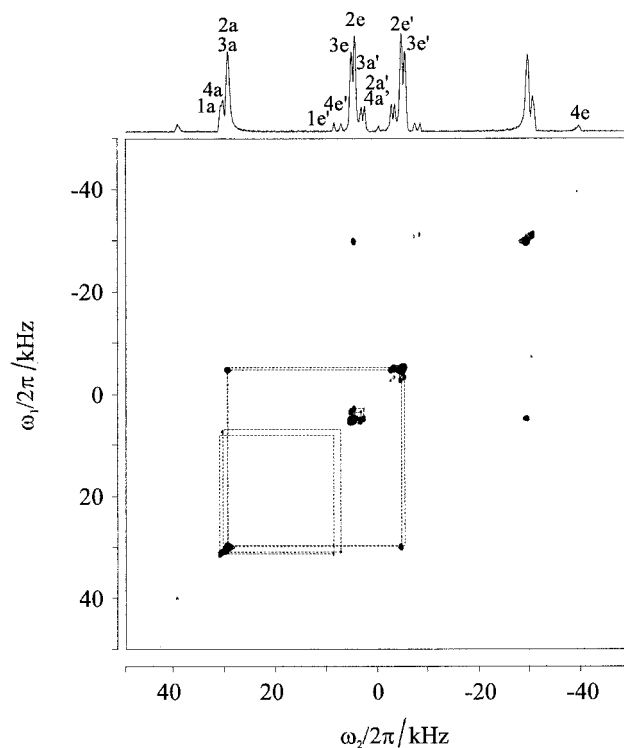


Figure 9. 2D exchange  $^2\text{H}$  NMR spectrum of iodocyclohexane- $\text{d}_{11}$ , recorded at 238 K with a mixing time of 3 ms.

system are required for a complete description of the experimental  $^2\text{H}$  NMR spectra [21–23]. One axis of the molecular-fixed coordinate system, the  $z'$ -axis, must be perpendicular to the molecular symmetry plane. For convenience the  $x'$ -axis is in the plane given by the carbon atoms C-2, C-3, C-5 and C-6 and perpendicular to the  $z'$ -axis (see figure 1). The  $z$ -axis of the principal coordinate system of the ordering matrix is collinear with the  $z'$ -axis. The remaining principal axes  $x$  and  $y$  lie in the  $x'y'$  plane, rotated about  $z = z'$  by the angle  $\alpha$ . In the  $x, y, z$  coordinate system the averaged quadrupolar interaction—corresponding to half of the experimental  $^2\text{H}$  NMR doublet—of a particular deuteron  $i$  is given by [21–23]

$$\langle v_Q^i \rangle = v_Q^i S_{xx} \left[ \frac{1}{2} (3 \cos^2 \theta_x^i - 1) + \frac{1}{2} \eta (\cos^2 \theta_z^i - \cos^2 \theta_y^i) \right] \quad (1)$$

where an axially symmetric quadrupolar coupling tensor has been assumed.  $v_Q^i$  is 3/4 of the static quadrupolar coupling constant  $e^2 q Q/h$ . In the present case a value of 168 kHz has been used that is typical for aliphatic deuterons. The angles  $\theta_y^i$  explicitly depend on  $\alpha$  and describe the orientation between the C–D $^i$  bond direction and the principal axis  $y$ . The asymmetry parameter  $\eta$  is



defined by  $\eta = (S_{zz} - S_{yy})/S_{xx}$ . For a theoretical description of the experimental  $^2\text{H}$  NMR doublets—apart from the molecular coordinates—the parameters  $S_{xx}$ ,  $\eta$  and  $\alpha$  are required.

In the first step of the analysis the molecular coordinates were determined from MM2 calculations [33]. Next, the angles  $\theta_\gamma^i$  were calculated by taking a particular angle  $\alpha$ . Inserting the values of  $\theta_\gamma^i$  along with distinct values for  $S_{xx}$  and  $\eta$  into equation (1) yielded a theoretical value for  $\langle v_Q^i \rangle$ .  $S_{xx}$ ,  $\eta$  and  $\alpha$  were then varied until the differences between the theoretical and experimental splittings were minimized. It should be noted that it was also necessary to check the different relative signs of the experimental values of  $\langle v_Q^i \rangle$  which are given by the cross peaks in the 2D exchange NMR experiments. The restriction of  $S_{xx}$  to be positive ensured that the molecular long axis is connected with a positive order parameter [21–25].

During the present work we started with the analysis of the  $^2\text{H}$  NMR spectra of the selectively deuteriated compounds, since here the number of possibilities for the assignment of the various signals was limited. In the final step the remaining signals of the perdeuteriated samples were assigned. The above analysis was first performed for the measurements at low temperature at  $T = 238$  K, taking into account both 1D  $^2\text{H}$  NMR lineshapes and 2D exchange  $^2\text{H}$  NMR spectra. Here, the quadrupolar doublets for each conformer could be taken directly from the experimental NMR spectra, since the ring inversion is on the slow time scale. At higher temperatures the splittings were taken from the input parameters of the lineshape simulations for the ring inversion process. Plots of the quadrupolar interactions  $\langle v_Q^i \rangle$  for both conformers as a function of temperature are given in figures 10 and 11. The final order parameters  $S_{\gamma\gamma}$ , asymmetry parameters  $\eta$  and angles  $\alpha$  are reported in tables 3 and 4. Figures 12 and 13 show the derived  $S_{\gamma\gamma}$  values as functions of temperature. In addition, the final assignments are depicted in the 2D exchange NMR spectra of figures 4, 6 and 9.

The data reveal a pronounced influence of the particular conformational state on the ordering features of chloro- and iodo-cyclohexane. That is, the axial conformers generally possess lower order parameters  $S_{\gamma\gamma}$  and larger values of  $\eta$  and  $\alpha$ , reflecting a more globular shape of this conformational state. On the contrary, the equatorial conformers are characterized by smaller  $\alpha$  and larger  $S_{xx}$  values which support the assumed elongated shape of these species. Here, the main ordering axis is almost collinear with the C-1/C-4 axis. These findings are in line with the available data for other cyclohexane derivatives of similar molecular structure. The ordering characteristics of the equatorial conformers of the present halocyclohexanes are very close to those reported

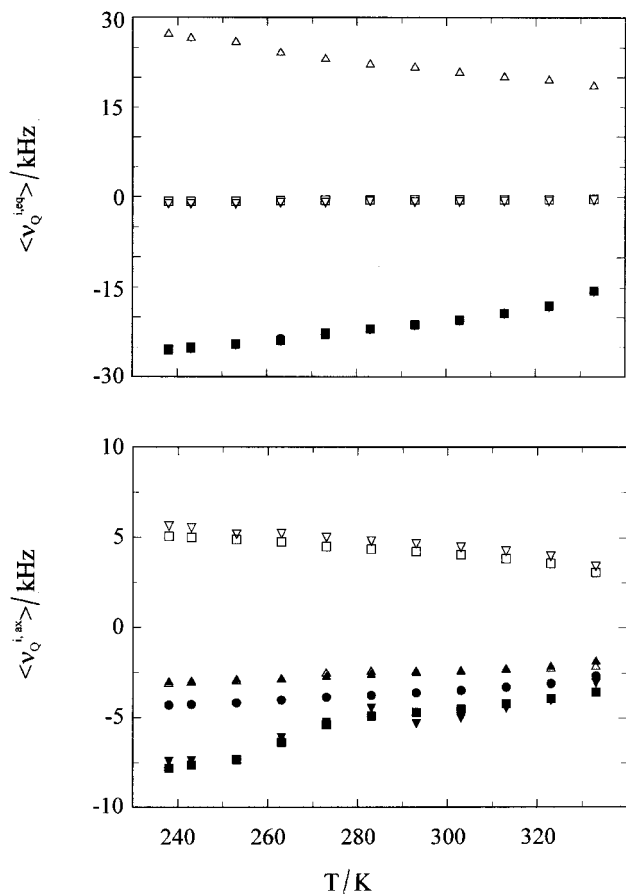


Figure 10. Experimental quadrupolar interactions  $\langle v_Q^i \rangle$  (half of the experimental splitting) for the various deuterons in the equatorial (upper figure) and axial (lower figure) conformer of chlorocyclohexane. Upper plot: D-1a ●; D-2e □; D-2a ■; D-3e ▽; D-3a ▲; D-4e △; D-4a ▲. Lower plot: D-1e' ●; D-2e' □; D-2a' ■; D-3e' ▽; D-3a' ▼; D-4e' △; D-4a' ▲.

earlier for bromo-, methyl- and 1,4-*cis*-dimethyl-cyclohexane [22, 23, 25]. Obviously, the polarity of the substituent is of minor importance. Rather, the comparison of the data for chloro-, bromo- [25] and iodo-cyclohexane reveals an effect by the atomic diameter of the halogen substituent. Consequently, the equatorial conformer  $S_{xx}$  increases from chloro- to iodo-cyclohexane, while  $\alpha$  decreases in the same direction. For instance, at 238 K  $S_{xx}$  varies from 0.251 through 0.294 to 0.330, on going from the chloro to the iodo substituent. At the same time,  $\alpha$  changes from 17.5 through 14.0 to 8.75. These parameters are consistent with the expected increase in aspect ratio of the equatorial conformers on moving towards the iodo substituent.

The axial conformation is characterized by a decrease of  $S_{xx}$  (at  $T = 238$  K: 0.262 (Cl), 0.140 (Br), 0.103 (I)), an increase of  $\alpha$  (at  $T = 238$  K: 51.5° (Cl), 53.2° (Br), 59.0° (I)) and an increase of  $\eta$  (at  $T = 238$  K: 0.46 (Cl),

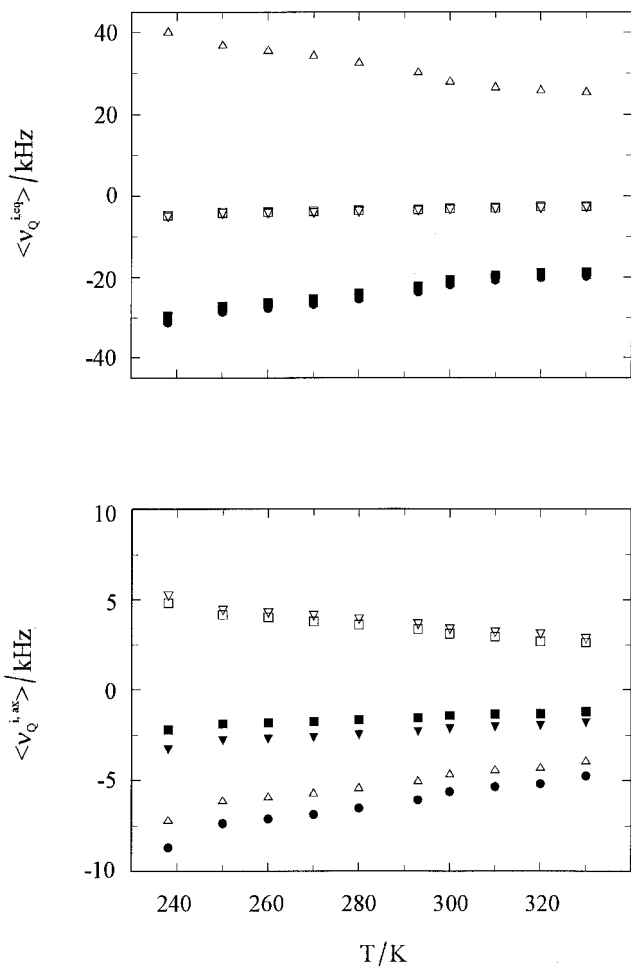


Figure 11. Experimental quadrupolar interactions  $\langle v_Q^i \rangle$  (half of the experimental splitting) for the various deuterons in the equatorial (upper figure) and axial (lower figure) conformer of iodocyclohexane; Upper plot: D-1a ●; D-2e □; D-2a ■; D-3e ▽; D-3a ▼; D-4e △; D-4a ▲. Lower plot: D-1e' ●; D-2e' □; D-2a' ■; D-3e' ▽; D-3a' ▼; D-4e' △; D-4a' ▲ (note: D-2a' and D-4a' exhibit the same splittings).

0.79 (Br), 1.15 (I)) with increasing size of the halogeno substituent, reflecting the tendency towards a more globular molecular shape. Furthermore,  $\eta$  is found to exhibit a strong temperature dependence for chlorocyclohexane, while  $\eta$  remains almost temperature independent for bromo- and iodo-cyclohexane. The origin of this latter result is so far unknown.

### 3.3. Conformational order and ring dynamics

As mentioned earlier, the equatorial and axial conformers of both cyclohexane derivatives exist in a dynamic equilibrium. The observed  $^2\text{H}$  NMR lineshape changes are a direct consequence of the mutual exchange between both conformational states in the liquid crystalline solvent ZLI 2452. At low temperatures ( $T = 238$  K),

Table 3. Derived order parameters  $S_{\gamma\gamma}$ , asymmetry parameters  $\eta$  and angles  $\alpha$  for both conformers of chlorocyclohexane in ZLI 2452.

| Temperature/K               | $S_{xx}^a$ | $S_{yy}^a$ | $S_{zz}^a$ | $\eta$ | $\alpha/^\circ$ |
|-----------------------------|------------|------------|------------|--------|-----------------|
| <i>Equatorial conformer</i> |            |            |            |        |                 |
| 238                         | 0.251      | -0.191     | -0.060     | 0.52   | 17.5            |
| 243                         | 0.264      | -0.195     | -0.069     | 0.48   | 19.2            |
| 253                         | 0.253      | -0.189     | -0.065     | 0.49   | 18.8            |
| 263                         | 0.285      | -0.215     | -0.065     | 0.51   | 19.6            |
| 273                         | 0.277      | -0.209     | -0.070     | 0.55   | 18.4            |
| 283                         | 0.238      | -0.190     | -0.068     | 0.60   | 17.2            |
| 292                         | 0.232      | -0.176     | -0.048     | 0.52   | 19.2            |
| 303                         | 0.222      | -0.169     | -0.056     | 0.52   | 19.2            |
| 313                         | 0.202      | -0.147     | -0.053     | 0.46   | 20.4            |
| 323                         | 0.169      | -0.125     | -0.044     | 0.48   | 18.4            |
| 333                         | 0.146      | -0.098     | -0.048     | 0.34   | 18.8            |
| <i>Axial conformer</i>      |            |            |            |        |                 |
| 238                         | 0.262      | -0.191     | -0.071     | 0.46   | 51.5            |
| 243                         | 0.250      | -0.184     | -0.066     | 0.47   | 51.7            |
| 253                         | 0.223      | -0.169     | -0.055     | 0.51   | 51.8            |
| 263                         | 0.209      | -0.158     | -0.051     | 0.51   | 52.4            |
| 273                         | 0.187      | -0.144     | -0.043     | 0.54   | 52.8            |
| 283                         | 0.168      | -0.131     | -0.037     | 0.56   | 52.9            |
| 292                         | 0.153      | -0.122     | -0.031     | 0.60   | 52.9            |
| 303                         | 0.133      | -0.111     | -0.022     | 0.67   | 52.8            |
| 313                         | 0.125      | -0.107     | -0.017     | 0.72   | 52.8            |
| 323                         | 0.107      | -0.093     | -0.014     | 0.74   | 52.8            |
| 333                         | 0.098      | -0.088     | -0.010     | 0.80   | 53.2            |

<sup>a</sup> Estimated errors:  $\pm 4\%$ .

Table 4. Derived order parameters  $S_{\gamma\gamma}$ , asymmetry parameters  $\eta$  and angles  $\alpha$  for both conformers of iodocyclohexane in ZLI 2452.

| Temperature/K               | $S_{xx}^a$ | $S_{yy}^a$ | $S_{zz}^a$ | $\eta$ | $\alpha/^\circ$ |
|-----------------------------|------------|------------|------------|--------|-----------------|
| <i>Equatorial conformer</i> |            |            |            |        |                 |
| 238                         | 0.330      | -0.251     | -0.079     | 0.52   | 8.75            |
| 250                         | 0.295      | -0.227     | -0.053     | 0.54   | 8.25            |
| 260                         | 0.287      | -0.219     | -0.053     | 0.52   | 8.75            |
| 270                         | 0.277      | -0.210     | -0.038     | 0.52   | 8.75            |
| 280                         | 0.271      | -0.206     | -0.055     | 0.52   | 8.75            |
| 290                         | 0.247      | -0.184     | -0.051     | 0.49   | 9.75            |
| 300                         | 0.227      | -0.171     | -0.053     | 0.51   | 9.25            |
| 310                         | 0.213      | -0.164     | -0.051     | 0.54   | 8.25            |
| 320                         | 0.211      | -0.157     | -0.054     | 0.49   | 9.75            |
| 330                         | 0.204      | -0.152     | -0.070     | 0.49   | 9.75            |
| <i>Axial conformer</i>      |            |            |            |        |                 |
| 238                         | 0.103      | -0.111     | 0.008      | 1.15   | 59.0            |
| 250                         | 0.088      | -0.094     | 0.007      | 1.15   | 59.0            |
| 260                         | 0.085      | -0.091     | 0.006      | 1.15   | 59.0            |
| 270                         | 0.082      | -0.088     | 0.006      | 1.15   | 59.0            |
| 280                         | 0.079      | -0.084     | 0.005      | 1.14   | 59.0            |
| 290                         | 0.072      | -0.078     | 0.005      | 1.15   | 59.0            |
| 300                         | 0.066      | -0.071     | 0.005      | 1.16   | 59.0            |
| 310                         | 0.063      | -0.068     | 0.005      | 1.16   | 59.0            |
| 320                         | 0.061      | -0.066     | 0.005      | 1.16   | 59.0            |
| 330                         | 0.056      | -0.061     | 0.004      | 1.16   | 59.0            |

<sup>a</sup> Estimated errors:  $\pm 4\%$ .

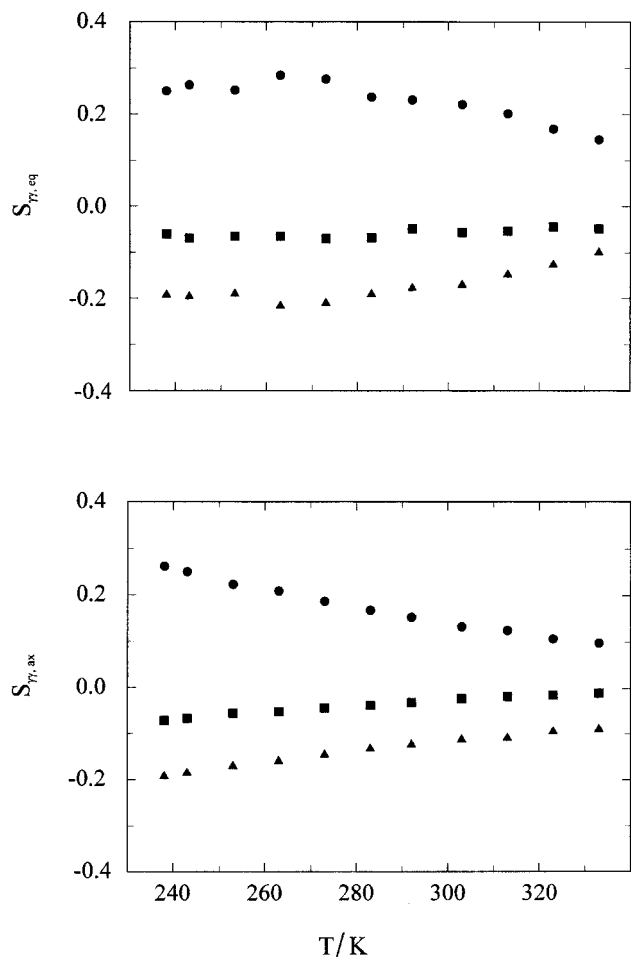


Figure 12. Plots of derived molecular order parameters  $S_{\gamma\gamma}$  as functions of temperature for the equatorial (top) and axial conformers (bottom) of chlorocyclohexane, respectively ( $S_{xx}$  ●;  $S_{yy}$  ▲;  $S_{zz}$  ■).

the underlying ring inversion process is slow on the NMR time scale. Here, the relative populations of the two conformers can be taken directly from the experimental spectra, yielding values of  $p_e = 0.72$  and  $0.73$  for chlorocyclohexane and iodocyclohexane, respectively. These values can be compared with those from former  $^1\text{H}$  NMR studies on isotropic solutions [37–39] which revealed a relatively weak temperature dependence of the conformational ratios for such cyclohexane derivatives [38, 39]. Höfner *et al.* [38] provided data for fluoro-, chloro- and bromo-cyclohexane. In the case of chlorocyclohexane, an exact agreement with our value of  $p_e = 0.72$  has been observed. Likewise, the value of  $p_e = 0.73$  for iodocyclohexane from our present study matches the reported value for bromocyclohexane in isotropic solution in the work by Höfner *et al.* On the other hand, it should be noted that the populations  $p_e$  reported by Bugay *et al.* [39] generally are somewhat lower

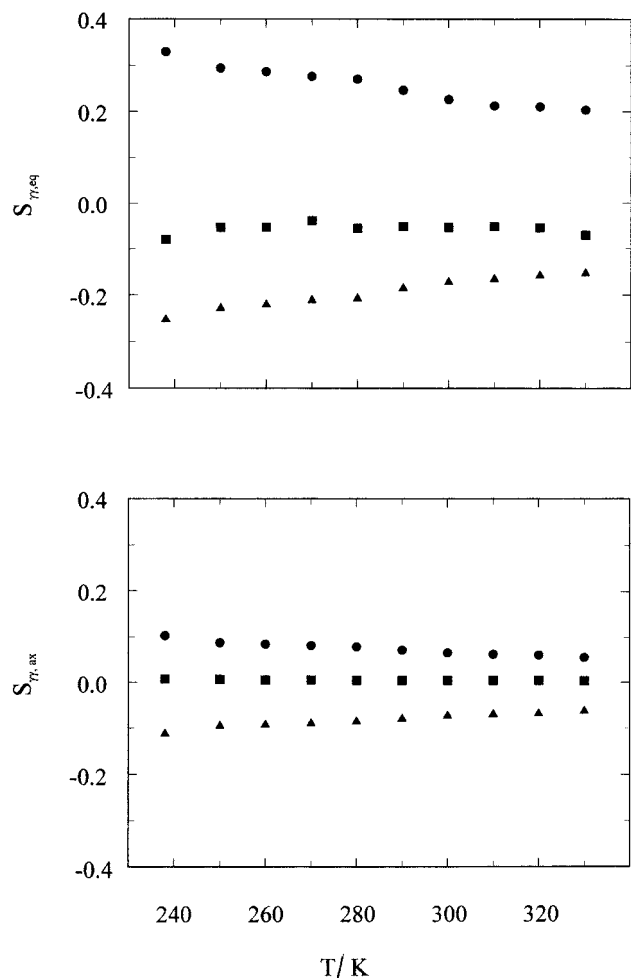


Figure 13. Plots of derived molecular order parameters  $S_{\gamma\gamma}$  as functions of temperature for the equatorial (top) and axial conformers (bottom) of iodocyclohexane, respectively ( $S_{xx}$  ●;  $S_{yy}$  ▲;  $S_{zz}$  ■).

( $\Delta p_e \sim 0.05$ ) as compared with Höfner's [38] and our own NMR work. Nevertheless, it is justified to state that the conformational equilibria of such halogeno substituted cyclohexanes are unaffected by the liquid crystalline matrix.

In the intermediate and fast exchange regions, the conformational ratios could not be determined independently from our present NMR data. In this region the populations of the chlorocyclohexane conformers were derived from the thermodynamic data, given by Höfner *et al.* [38]. In the case of iodocyclohexane, the conformational ratios were derived from the thermodynamic data provided for bromocyclohexane in the same work. This assumption appears to be justified, since—as mentioned above—at low temperatures both data sets exhibit good agreement, while the data for iodocyclohexane provided by Bugay *et al.* [39] were constantly shifted towards lower values for  $p_e$ .

The lineshape simulations were done by varying the rate constant of the ring inversion process and the quadrupolar splittings of each exchanging signal pair. Furthermore, an exchange and temperature independent linewidth was used which varied between 175 and 860 Hz for the various deuterons. The final best fit simulations are given in the right hand columns of figures 3, 5, 7 and 8. The rate constants  $1/\tau$  ( $=k_a + k_e = k_e/p_a = k_a/p_e$ ) for the ring inversion process are summarized in the Arrhenius plots of figure 14. The derived activation enthalpies of  $\Delta H = 48.1 \pm 1.0$  and  $40.6 \pm 2.3$  kJ mol<sup>-1</sup> for chloro- and iodo-cyclohexane, respectively, are found to be very close to those reported from other studies of this process for the isotropic solution [37], implying a minor influence of the liquid crystalline solvent on the internal ring inversion process. This is in line with other studies on related systems where the conformational properties—comprising conformational order and dynamics—remain unaffected by the liquid crystalline matrix [21–25].

#### 4. Summary

Dynamic <sup>2</sup>H NMR methods were used to study selectively and perdeuterated samples of bromo- and iodo-cyclohexane in a liquid crystalline matrix. It was found that for both molecules the axial and equatorial conformers exist in a dynamic equilibrium which can be studied adequately employing dynamic <sup>2</sup>H NMR techniques. The lineshape analysis of the variable temperature <sup>2</sup>H NMR spectra provided the conformational ratios and kinetic parameters of the ring inversion process which were found to be almost unaffected by the nematic solvent. Analysis of variable temperature <sup>2</sup>H NMR lineshapes and 2D exchange <sup>2</sup>H NMR spectra

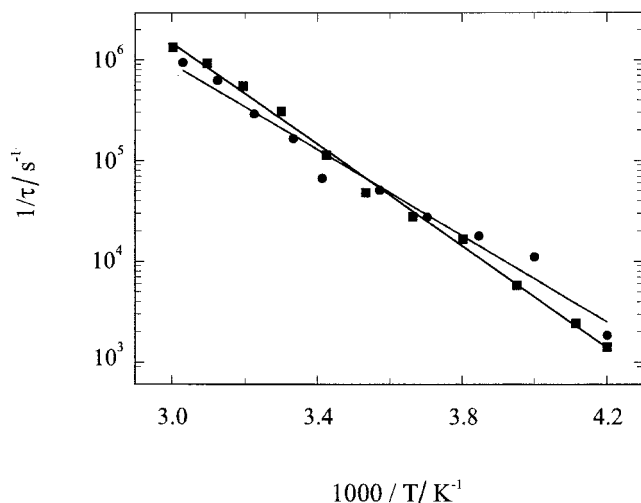


Figure 14. Arrhenius representation for the rate constants of the ring inversion process of chlorocyclohexane ■, and iodicyclohexane ●, in ZLI 2452.

gave access to the ordering characteristics of chloro- and iodo-cyclohexane. The derived order parameters have demonstrated a strong influence by the actual conformational state which can be traced back to the overall shape of the individual conformers. The same holds for the size of the substituent, while its polarity obviously is of minor importance for the molecular order parameters of such cyclohexane derivatives.

We thank Mrs H. Seidel for help during the synthesis of the deuterated compounds used in the present study. Financial support by the Deutsche Forschungsgemeinschaft and the Fonds der Chemischen Industrie is gratefully acknowledged.

#### References

- [1] EMSLEY, J. W., and LINDON, J. C., 1975, *Nuclear Magnetic Resonance Spectroscopy using Liquid Crystal Solvents*, (New York: Pergamon).
- [2] EMSLEY, J. W., 1985, *Nuclear Magnetic Resonance of Liquid Crystals* (Dordrecht: D. Reidel).
- [3] DONG, R. Y., 1994, *Nuclear Magnetic Resonance of Liquid Crystals* (New York: Springer-Verlag).
- [4] GOLDFARB, D., LUZ, Z., and ZIMMERMANN, H., 1983, *Israel J. Chem.*, **23**, 341.
- [5] HSI, S., ZIMMERMANN, H., and LUZ, Z., 1978, *J. chem. Phys.*, **69**, 4126.
- [6] PHOTINOS, D. J., BOS, P. J., DOANE, J. W., and NEUBERT, M. E., 1979, *Phys. Rev.*, **20**, 2203.
- [7] BODEN, N., BUSHBY, R. J., and CLARK, L. D., 1979, *Chem. Phys. Lett.*, **64**, 519.
- [8] DONG, R. Y., and SAMULSKI, E. T., 1982, *Mol. Cryst. liq. Cryst.*, **82**, 73.
- [9] BODENHAUSEN, G., SZEVEHENYI, N. M., VOLD, R. L., and VOLD, R. R., 1978, *J. Am. chem. Soc.*, **100**, 6265.
- [10] GOLDFARB, D., BELSKY, I., LUZ, Z., and ZIMMERMANN, H., 1983, *J. chem. Phys.*, **79**, 6203.
- [11] HOATSON, G. L., BAILEY, A. L., VAN DER EST, A. J., BATES, G. S., and BURNELL, E. E., 1988, *Liq. Cryst.*, **3**, 683.
- [12] SAMULSKI, E. T., 1980, *Ferroelectrics*, **30**, 83.
- [13] BURNELL, E. E., and DE LANGE, C. A., 1998, *Chem. Rev.*, **98**, 2359.
- [14] DIEHL, P., and KHETRAPAL, C. L., 1969, in *NMR, Basic Principles and Progress*, Vol. 1, edited by P. Diehl, E. Fluck and R. Kosfeld (Berlin: Springer-Verlag), p. 1.
- [15] SURYAPRAKASH, N., UGOLINI, R., and DIEHL, P., 1991, *Magn. Reson. Chem.*, **29**, 1024.
- [16] EMSLEY, J. W., 1985, in *Nuclear Magnetic Resonance of Liquid Crystals*, edited by J. W. Emsley (Dordrecht: D. Reidel), p. 379.
- [17] FUNG, B. M., AFZAL, J., FOSO, T. L., and CHAU, M.-H., 1986, *J. chem. Phys.*, **85**, 4808.
- [18] GUO, W., and FUNG, B. M., 1991, *Liq. Cryst.*, **9**, 117.
- [19] POUPKO, R., and LUZ, Z., 1996, in *Encyclopedia of Nuclear Magnetic Resonance*, Vol. 3, edited by D. M. Grant and R. K. Harris (New York: John Wiley), p. 1783.
- [20] POUPKO, R., and LUZ, Z., 1981, *J. chem. Phys.*, **75**, 1675.

- [21] BOEFFEL, C., LUZ, Z., POUPKO, R., and ZIMMERMANN, H., 1990, *J. Am. chem. Soc.*, **112**, 7158.
- [22] MÜLLER, K., LUZ, Z., POUPKO, R., and ZIMMERMANN, H., 1992, *Liq. Cryst.*, **11**, 547.
- [23] TERZIS, A. F., POON, C.-D., SAMULSKI, E. T., LUZ, Z., POUPKO, R., ZIMMERMANN, H., MÜLLER, K., TORIUMI, H., and PHOTINOS, D. J., 1996, *J. Am. chem. Soc.*, **118**, 2226.
- [24] BOEFFEL, C., LUZ, Z., POUPKO, R., and VEGA, A., 1988, *Israel J. Chem.*, **28**, 283.
- [25] TERNIEDEN, S., MÜLLER, D., and MÜLLER, K., 1999, *Liq. Cryst.*, **26**, 759.
- [26] LOMPA-KRZYMIEN, L., and LEITCH, L. C., 1973, *J. Labelled Compd.*, **9**, 331.
- [27] ZIMMERMANN, H., 1989, *Liq. Cryst.*, **4**, 591.
- [28] GREEN, M. M., and SCHWAB, J., 1968, *Tetrahedron Lett.*, **25**, 2955.
- [29] PERLMAN, D., DAVIDSON, D., and BOGERT, M. T., 1936, *J. org. Chem.*, **1**, 288.
- [30] STONE, H., and SHECHTER, H., 1950, *J. org. Chem.*, **15**, 491.
- [31] SCHAEFER, D., LEISEN, J., and SPIESS, H. W., 1995, *J. magn. Res.*, **A115**, 60.
- [32] SCHMIDT, C., BLÜMICH, B., and SPIESS, H. W., 1988, *J. magn. Res.*, **79**, 269.
- [33] ALLINGER, N. L., 1977, *J. Am. chem. Soc.*, **99**, 8127; BURKERT, U., and ALLINGER, N. L., 1982, *Molecular Mechanics* (Washington: American Chemical Society).
- [34] DAMIANI, D., SCAPPINI, F., CAMINATI, W., and CORBELLI, G., 1983, *J. mol. Spectr.*, **100**, 36.
- [35] SHEN, Q., and PELOQUIN, J. M., 1988, *Acta Chem. Scan.*, **A42**, 367.
- [36] BIALKOWSKA-JAWORSKA, E., JAWORSKI, M., and KISIEL, Z., 1995, *J. mol. Struct.*, **350**, 247.
- [37] SUBBOTIN, O., and SERGEYEV, N. M., 1975, *J. Am. chem. Soc.*, **97**, 1080.
- [38] HÖFNER, D., LESKO, S., and BINSCH, G., 1978, *Org. magn. Res.*, **11**, 179.
- [39] BUGAY, D. E., BUSHWELLER, C. H., DANEHEY, C. T., HOOGASIAN, S., BLERSCH, J. A., and LEENSTRA, W. R., 1989, *J. phys. Chem.*, **93**, 3908.
- [40] SAUPE, A., 1964, *Z. Naturforsch. (a)*, **19**, 161.